

## Approximation of the lateral distribution function of the Cherenkov light from extensive air showers in the primary energy region 1–100 PeV

---

V. S. Latypova,<sup>a,b,\*</sup> C. G. Azra,<sup>a</sup> E. A. Bonvech,<sup>b</sup> D. V. Chernov,<sup>b</sup> V. I. Galkin,<sup>a,b</sup> V. A. Ivanov,<sup>a,b</sup> D. A. Podgrudkov<sup>a,b</sup> and T. M. Roganova<sup>b</sup>

<sup>a</sup>*Faculty of Physics, M.V. Lomonosov Moscow State University  
Leninskie gory, 1(3), Moscow, 119991, Russia.*

<sup>b</sup>*Skobeltsyn Institute for Nuclear Physics, M.V. Lomonosov Moscow State University  
Leninskie gory, 1(3), Moscow, 119991, Russia.*

*E-mail:* [latypova.vs17@physics.msu.ru](mailto:latypova.vs17@physics.msu.ru)

Cherenkov light lateral distribution function approximation that describes an individual extensive air shower was found. It is designed for showers from various primary nuclei in the 1–100 PeV energy range with zenith angles up to 20° and distances from the shower axis of up to 500 meters. Approximation accuracy is better than 10%. Initially, the approximation was intended for processing events of the SPHERE-2 experiment, but it can also be applied to any other experiment that uses the Cherenkov light lateral distribution function at the ground level. A comparison was made with simpler approximating functions used in the SPHERE-2 processing and in the TAIGA experiment.

\*\*\* 27th European Cosmic Ray Symposium - ECRS \*\*\*

\*\*\* 25-29 July 2022 \*\*\*

\*\*\* Nijmegen, the Netherlands \*\*\*

---

\*Speaker

## 1. Introduction

One of the main problems in cosmic ray physics is measurement of partial spectra from primary cosmic rays (PCR). PCR particles with energies of up to  $10^{15}$  eV can be detected by direct methods using detectors mounted on satellites [1] and high altitude balloons [2]. The intensity of ultra high energy particles (above  $10^{15}$  eV) is so low that all measurements at such energies are currently carried out by indirect methods based on the characteristics of extensive air showers (EASs).

For EAS measurements large ground detector arrays are most often used, for example, the Pierre Auger Observatory [3], TAIGA [4], the Telescope Array [5], the Yakutsk array [6, 7] and others. However, the SPHERE-2 experiment used the balloon-borne detector. It registered Vavilov–Cherenkov radiation (Cherenkov light, CL) reflected from the snow-covered ice of Lake Baikal. This registration method allows to obtain data on the CL intensity from the near-axial region of an EAS — the region which is most sensitive to the type of primary particle [8]. The detector was located at 1 km above the snow surface and observed an area of about 900 m in diameter.

One goal of the SPHERE-2 experiment was to estimate the PCR mass composition. The criteria for estimating the primary mass are based on the measured shape of the EAS CL lateral distribution function (LDF) and are defined as the ratio of Cherenkov photon numbers within the rings of different radii (up to 300 m). And since the shower core region, conventionally, from 0 to 100 m, carries important information on the primary particle mass, in order to extract the data on the PCR mass the LDF approximation should be fairly accurate in the whole range from 0 up to 300–400 m.

## 2. Generation and processing of simulated vertical EAS events

Events used for approximation were simulated using CORSIKA7.5600 [9]. Each event was modelled with the following primary parameters:

- primary particle energy (1, 10, 30, 100 PeV);
- shower incidence angle (10, 15, 20°);
- primary particle type (protons (p), nuclei: helium (He), nitrogen (N), iron (Fe));
- atmospheric model (two very different atmospheric models were considered: atmosphere No.1 - a standard American atmosphere approximated by J. Linsley, and No.11 - the South Pole atmosphere (MSIS-90-E) from CORSIKA);
- high energy hadron interaction model (QGSJET-01 [10], QGSJETII-04 [11]);
- observation level: set to the surface of Lake Baikal (455 m above the sea level).

Simulation resulted in arrays of  $1280 \times 1280$  cells,  $2.5 \times 2.5$  m<sup>2</sup> each, filled with Cherenkov photons coming from an individual EAS with given primary parameters. The array forms a  $3200 \times 3200$  m<sup>2</sup> data carpet centered on the shower axis, which characterizes the EAS CL LDF. LDF from showers with small zenith angles can be considered as axially symmetric — for an individual CL LDF variations in the relative photon counts within a thin ring of any given radius was on average 10%. By averaging the number of photons in cells located at the same distance from the shower axis a one dimensional LDF, which will further be used to analyze the approximations described below, is obtained.

### 3. Considered approximations of EAS CL LDF

Several approximations were considered in order to achieve a high enough accuracy of primary particle mass estimation criteria calculations.

#### 3.1 SPHERE-2 early approximation

Previously, in the SPHERE-2 experiment, an approximation which used a rational function for the form (1) was implemented. It was also used for the Pamir-XXI project [12].

$$F_{old}(p_0, p_1, p_2, R) = \frac{p_0}{(1 + p_1 \cdot R + p_2 \cdot R^2)} \quad (1)$$

The parameters were found using the MINUIT [13] package and the least squares method. The MINUIT package uses the gradient descent method to minimize the multi-parameter function  $FCN$  (2), which is defined as the sum of squared deviations of data points  $I(R)$  from the proposed approximating function  $F_{old}$ .

$$FCN(p_0, p_1, p_2) = \sum_R (I(R) - F_{old}(p_0, p_1, p_2, R))^2 \quad (2)$$

Figure 1a shows a LDF of an event originating from a 10 PeV proton with a  $15^\circ$  zenith angle in atmosphere model 1 with the QGSJETII-04 model. From the presented plot it can be seen that the errors  $d = (I(R) - F_{old})/I(R)$  increase with the distance from the shower axis and these errors are rather high. The relative deviation of the approximating curve from the simulated points is about 15% at distances below 200 meters from the shower axis. At distances above 300 meters, the errors exceed 50%. Therefore, another form of the approximation was considered, which was used earlier in the TAIGA experiment.

#### 3.2 The TAIGA approximation

An EAS CL LDF approximation which was used under similar conditions in the Tunka-25 experiment (their site was located near Lake Baikal at the same altitude) was taken from [14]. The coefficients are given with the corrections from the authors (provided in a private communication).

1. LDF steepness parameter:  $P = I(100)/I(200)$ , where  $I(100)$  is the number of photons at a distance of  $R = 100$  meters from the shower axis. The following 4 parameters depend on it:

$$R_0 = \exp(6.79 - 0.564 \cdot P) \quad (3)$$

$$R_{kn} = 207 - 24.5 \cdot P \quad (4)$$

$$b = \begin{cases} 4.8367 - 2.8261 \cdot \log(6.5 - P), & P < 6 \\ 4.8367 - 2.8261 \cdot \log(6.5 - 6), & P \geq 6 \end{cases} \quad (5)$$

$$Q_{kn} = I(175) \cdot \left( \frac{R_{kn}}{175} \right)^{-2.2} \quad (6)$$

2. Three different functions are used in three areas:

$$f(R_0, R_{kn}, b, R) = \begin{cases} \exp\left(\frac{R_{kn} - R}{R_0} \cdot \left(1 + \frac{3}{(R+3)}\right)\right), & 30 < R < R_{kn} \\ \left(\frac{R_{kn}}{R}\right)^{2.2}, & R_{kn} \leq R \leq 200 \\ \left(\frac{R_{kn}}{200}\right)^{2.2} \cdot \left(\frac{(R/200 + 1)}{2}\right)^{-b}, & R > 200 \end{cases} \quad (7)$$

3. Final function:

$$Q(R_0, R_{kn}, b, Q_{kn}, R) = Q_{kn} \cdot f(R_0, R_{kn}, b, R) \quad (8)$$

From the results presented on the right panel of fig. 1b it follows that the main error accumulates in the first 100 meters. But it is precisely this part that is significant for further processing of events, since the criteria for estimating the primary mass is essentially based on the LDF shape in the near-axial region. Therefore, again, another type of approximation was considered.

### 3.3 The new approximation of SPHERE-2

The CL LDF has a clear feature: the steepness of the function changes at around 70–150 meters from the shower axis (the specific value depends on the given primary parameters).

A class of rational approximations by a single function with a different number of parameters was considered. The LDF is described with high accuracy by a rational function in the section before the slope change and is also quite accurately described by a function of the same type in the section after that, but with different parameters. Thus an approximation (9) with weights (10) turned out to be accurate enough with a reasonable number of parameters.

$$F_{new} = \frac{p_0}{(1 + p_1 R + p_2 R^2 + p_3 R^3)} \times \omega_1 + \frac{p_4}{(1 + p_5 R + p_6 R^2)} \times \omega_2 \quad (9)$$

$$\begin{cases} \omega_1 = \frac{1}{(1 + \exp^{(R-R_{ch})/s})} \\ \omega_2 = \frac{1}{(1 + \exp^{-(R-R_{ch})/s})} \end{cases} \quad (10)$$

For  $R < R_{ch}$  :  $\omega_2 \ll 1$ , the first term, which is responsible for the region up to the slope change radius  $R_{ch}$ , is the most significant. For  $R > R_{ch}$  :  $\omega_1 \ll 1$ , the second term, which is responsible for the region after the slope change radius, is more significant. The optimal value of the parameter  $s = 8$  m was chosen so as not to clutter up the already multi-parameter function. The search for parameters was performed by the least squares method.

$$FCN(p_0, \dots, p_6, R_{ch}) = \sum_R (I(R) - F_{new}(p_0, \dots, p_6, R_{ch}, R))^2 \quad (11)$$

Characteristic initial values of the approximation parameters were the following:  $p_0 = 10^7$  photon  $m^{-2}$ ,  $p_1 = 0.1$   $m^{-1}$ ,  $p_2 = -0.001$   $m^{-2}$ ,  $p_3 = 10^{-5}$   $m^{-3}$ ,  $p_4 = 5 \cdot 10^5$  photon  $m^{-2}$ ,  $p_5 = -0.01$   $m^{-1}$ ,  $p_6 = 6 \cdot 10^{-5}$   $m^{-2}$ ,  $R_{ch} = 160$  m.

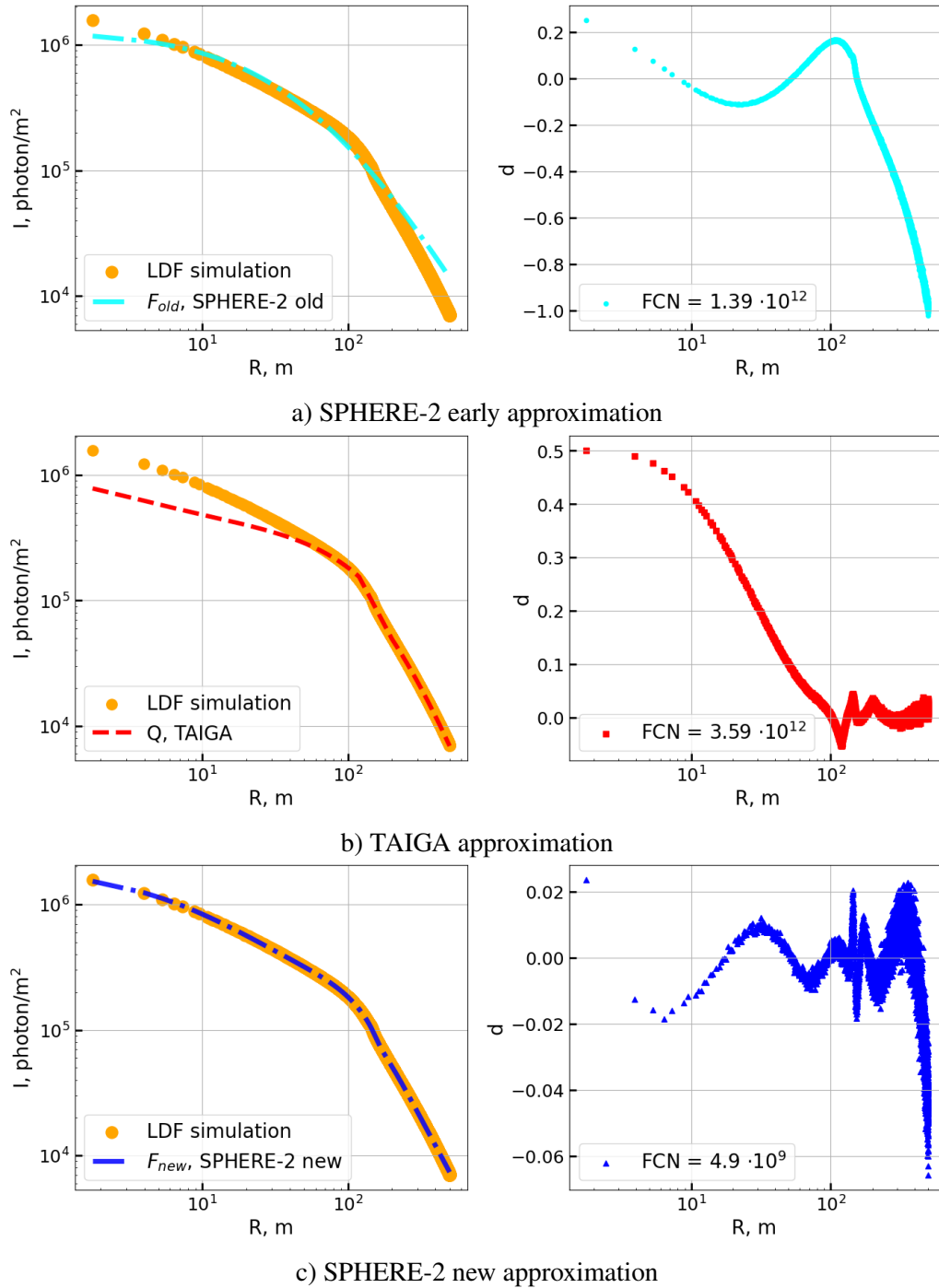


**Figure 1:** Approximations for a 10 PeV proton CL LDF with a zenith angle  $15^\circ$  in atmosphere model 1, QGSJETII-04 model. Left panels show the LDF data: orange dots stand for the simulation data, curves denote the approximations. Right panels show the relative deviations of the curves from the points. Pair a) shows the old SPHERE-2 approximation data, pair b) describes the TAIGA approximation, and pair c) deals with the new SPHERE-2 approximation. FCN values in the point of minimum indicate the quality of approximation.

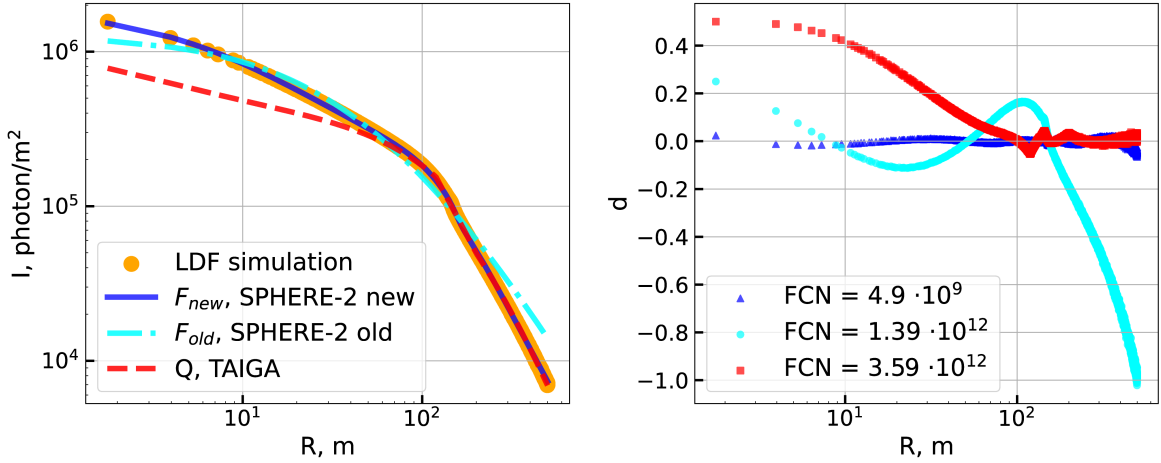


**Figure 2:** Left panel shows the LDF data: orange dots stand for the simulation data, curves denote the corresponding approximations. Right panel shows the relative deviation of the curves from the points. FCN values in the point of minimum indicate the quality of approximation.

Figure 1c shows the approximation by the new function (9). From the presented plot it can be seen that errors increase with the distance and do not exceed 7% up to 500 m from the shower axis for the selected individual simulated event.

### 3.4 Approximation comparison

In fig. 2, a graph is presented, which displays all of the approximations considered above. Among them, the  $F_{new}$  function has the smallest relative errors in the 0–500 m range. The value of the FCN function at the minimum is the smallest for  $F_{new}$ . This trend persists for other primary parameters as well.

In fig. 3 EAS LDFs of simulated events and the corresponding approximations by the new function  $F_{new}$  for various primary parameters are presented:

- Fig. 3a — various primary particles with an energy of  $E = 30$  PeV,  $15^\circ$  zenith angle, atmosphere model 1, QGSJETII-04 interactions model;
- Fig. 3b — different energies of the primary proton,  $15^\circ$  zenith angle, atmosphere model 1, QGSJETII-04 interactions model;
- Fig. 3c — different zenith angles of a 10 PeV primary proton in atmosphere model 1 with the QGSJETII-04 interactions model;
- Fig. 3d — various interaction models for showers from a 10 PeV primary proton with a  $15^\circ$ s zenith angle in the atmosphere model 1.

The new approximation  $F_{new}$  in the 2–400 meters area deviates from the simulated LDF by no more than 2%, and changes in the primary parameters do not affect the overall quality of the approximation.

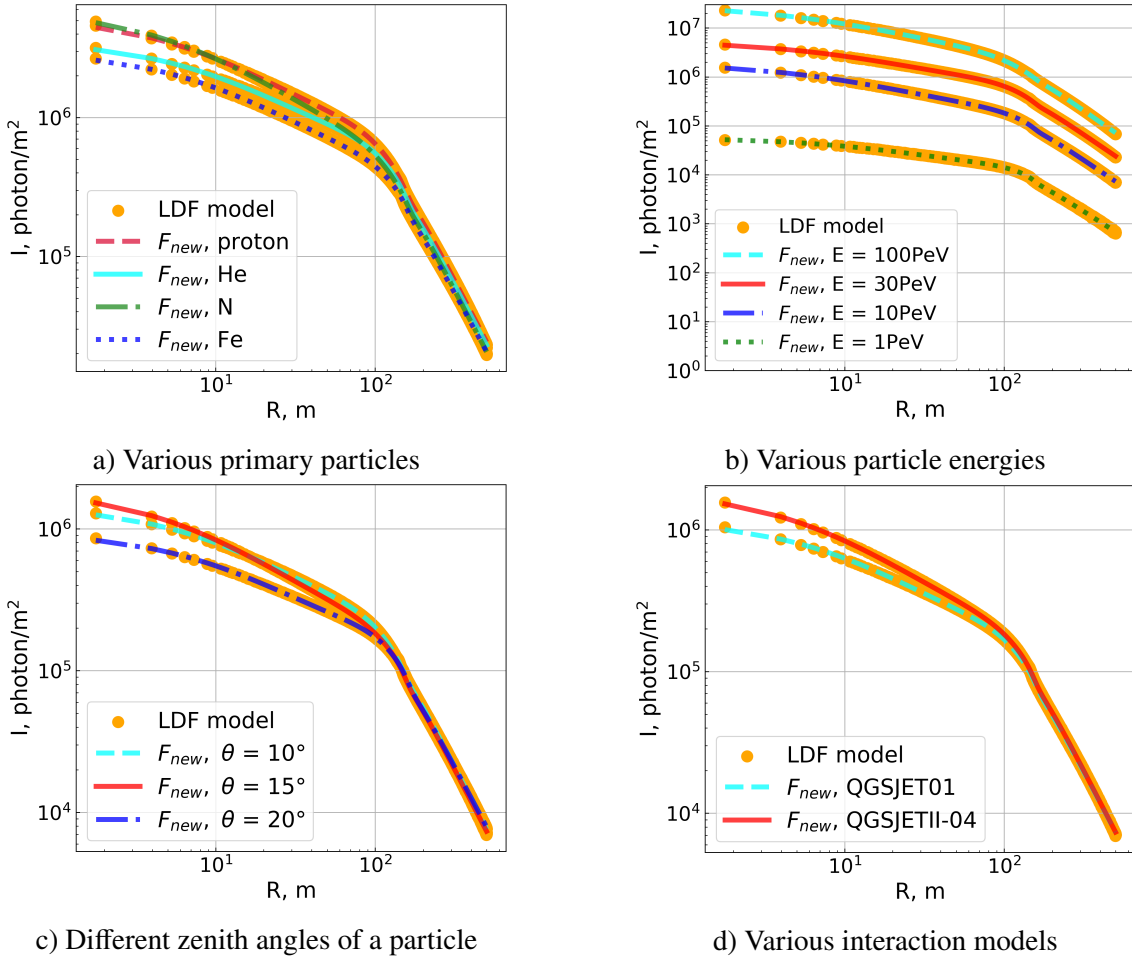


**Figure 3:** LDF data: orange dots stand for the simulation data, curves denote the corresponding approximations. Graph a) shows LDF for various primary particles, graph b) for various particle energies, graph c) for different zenith angles of a particle, graph d) for various interaction models.

#### 4. Conclusion

Function  $F_{new}$  approximates the EAS CL LDF and deviates from the simulated data by less than 10% within the 500 m distance from the shower axis. The approximation has been verified in the energy range of 1–100 PeV, at 455 meters above sea level, for shower zenith angles not exceeding  $20^\circ$  (fig. 3). For the majority of events at distances within the 2–400 m range the approximation error does not exceed 2% (fig. 1c). At distances beyond 400 m, an increase in the error is observed, depending on the considered individual EAS event, the deviation can reach up to 10%. However, such an increase in the error is not critical, since it is the region near the shower axis that is the most important for primary mass estimation. The presented approximation makes it possible to increase the accuracy of subsequent analysis, such as the estimation of the primary particle energy, as well as its mass.

## References

- [1] D. Podorozhny, V. Grebenyuk, D. Karmanov, I. Kovalev, I. Kudryashov, A. Kurganov et al., *Review of the results from the NUCLEON space mission*, *Advances in Space Research* **70** (2022) 1529.
- [2] V.A. Derbina, V.I. Galkin, M. Hareyama, Y. Hirakawa, Y. Horiuchi, M. Ichimura et al., *Cosmic-Ray Spectra and Composition in the Energy Range of 10–1000 TeV per Particle Obtained by the RUNJOB Experiment*, *The Astrophysical Journal* **628** (2005) L41.
- [3] J. Stasielak, *AugerPrime - The upgrade of the Pierre Auger Observatory*, *International Journal of Modern Physics A* **37** (2022) 2240012 [2110.09487].
- [4] D.V. Chernov, E.E. Korosteleva, V.V. Kuzmichev, L. A. and Prosin, I.V. Yashin, N.M. Budnev, O.A. Gress et al., *Primary energy spectrum and mass composition determined with the Tunka EAS Cherenkov array*, *International Journal of Modern Physics A* **20** (2005) 6799.
- [5] H. William, *Telescope array 10 year composition*, *Proc. of the 36<sup>th</sup> Int. Cosmic Ray Conf.* (2019) 280 [1908.01356].
- [6] A. Ivanov, *The Yakutsk Array Experiment: Main Results and Future Directions*, *EPJ Web of Conf.* **53** (2013) 04003.
- [7] A.K. Alekseev, E.A. Atlasov, N.G. Bolotnikov, A.V. Bosikov, N.A. Dyachkovskiy, N.S. Gerasimova et al., *Status of the Yakutsk Air Shower Array and Future Plans*, *Physics of Atomic Nuclei* **84** (2021) 893 [2107.07528].
- [8] R. Antonov, E. Bonvech, D. Chernov, T. Dzhatdov, V. Galkin, D. Podgrudkov et al., *Spatial and temporal structure of EAS reflected Cherenkov light signal*, *Astroparticle Physics* **108** (2019) 24.
- [9] D. Heck, J. Knapp, J.N. Capdevielle, G. Schatz and T. Thouw, *CORSIKA: A Monte Carlo code to simulate extensive air showers*, (1998) Report FZKA.
- [10] P.A. Kalmykov N.N., Ostapchenko S.S., *Quark-gluon string model and EAS simulation problems at ultra-high energies*, *Nucl. Phys. B (Proc. Suppl.)* **52** (1997) 17.
- [11] S. Ostapchenko, *Lhc data on inelastic diffraction and uncertainties in the predictions for longitudinal eas development*, *Physical Review D* **89** (2014) 074009.
- [12] V.I. Galkin, A. Borisov, R. Bakhromzod, V.V. Batraev, S.Z. Latipova and A.R. Muqumov, *A method for estimation of the parameters of the primary particle of an extensive air shower by a high-altitude detector*, *Moscow University Physics Bulletin* **73** (2018) 179.
- [13] F. James, *MINUIT Function Minimization and Error analysis*, CERN Geneva, Switzerland **94** (1994) .
- [14] N. Budnev, D. Chernov, O. Gress, E. Korosteleva, L. Kuzmichev, B. Lubsandorzhev et al., *Tunka-25 air shower cherenkov array: The main results*, *Astroparticle Physics* **50–52** (2013) 18.